45th AIAA/ASME/ASCE/AHS/ASC Structures, Structural Dynamics & Materials Conference
19 - 22 April 2004, Palm Springs, California

AIAA 2004-2034

Simulation Model of an Autonomous Underwater Vehicle for Design Optimization

Neal M. Patel * Shawn E. Gano† John E. Renaud ‡
University of Notre Dame, Notre Dame, Indiana, 46556
Jay D. Martin§ Michael A. Yukish¶
Applied Research Laboratory, State College, Pennsylvania, 16805

In this research, a stochastic simulation based design tool that facilitates design in a dynamic environment is developed. The simulation includes a full dynamic model of an Autonomous Underwater Vehicle (AUV) that was developed to evaluate the effectiveness of such a craft given a set of physical attributes. These attributes include but are not limited to: speed, mass, moments of inertia, control gains in the auto-pilot, and target detection capabilities. The effectiveness of the AUV is based upon the probability that it can successfully complete a given mission and how quickly it can complete this mission. The model is coupled with the Applied Research Lab's unclassified AUV problem that can compute weights, speeds, and efficiencies based on propulsor types, sonar configurations, and various other subsystems. In order to use this model in an optimization framework a mission was selected. This mission was to hit an oncoming torpedo before the torpedo was able to hit its target. The objective of this mission was to maximize the probability of successfully hitting the torpedo before the torpedo reaches its own target. In order to calculate this probability, the simulation was run with many different starting configurations including: different speeds of the oncoming torpedo, evasive maneuvers of the oncoming torpedo, and also various spacial orientations between the AUV and the targeted torpedo. This paper includes a detailed description of the simulation model, the development of the multidisciplinary design problem, and results obtained from the optimization of this problem.

Nomenclature

α	Angle of attack
β	Side slip angle
δ	Fin deflection
ρ	Density of surrounding fluid
ϕ, θ, ψ	Euler angles
$\widehat{b}$	Body-fixed reference frame
D	Drag
g	Gravitational acceleration
l	Vehicle total length
m	Vehicle total mass
r	Vehicle radius
V	Velocity
p, q, r	Rotational velocities

*Graduate Research Assistant, Aerospace and Mechanical Engineering, e-mail: npatel@nd.edu, Student Member AIAA
†Graduate Research Assistant, Aerospace and Mechanical Engineering, e-mail: sgano@nd.edu, Student Member AIAA
‡Professor, Aerospace and Mechanical Engineering, e-mail: jrenaud@nd.edu, Associate Fellow AIAA.
§Research Assistant, Product & Process Design Department, e-mail: jdm111@psu.edu, member AIAA.
¶Head, Product & Process Design Department, e-mail: may106@psu.edu, member AIAA

u, v, w	Body-fixed velocities
x_{bow}	Aft end of bow section
x_{bow2}	Forward end of bow section
x_{fin}	Aft end of fin section
x_{fin2}	Forward end of fin section
x_{tail}	Aft end of tail section
x_{tail2}	Forward end of tail section

I. Introduction

The Navy's Applied Research Laboratory at Penn State has developed an unclassified two variable design problem for an Autonomous Underwater Vehicle (AUV) that has proved to be overly simplistic and linear. In order to create a more credible model, a dynamic simulation model is developed in this research. The simulation model includes a six-degree of freedom dynamics model of a simple underwater vehicle, which referred to as the AUV, modeled in Mathworks' SIMULINK which is executed from MATLAB. This model includes added mass and cross terms as well as cross-flow drag to accurately model the nonlinear dynamics. The model is one big feedback loop that is driven by the evading vehicle's position relative to the pursuing vehicle and the subsequent pursuit.

To make the model more complex, simple differential game theory is integrated into the simulation by incorporating a pursuit game. The pursuer is the modeled vehicle that uses a simple autonomous controller to follow a target. This target is the evader, a non-dynamically modeled, unintelligent vehicle that travels on a programmed path. This vehicle can be launched at different orientations and depths. The pursuing vehicle first attempts to orient itself in the direction of the target to get a lock on it using its sonar. Subsequently, the vehicle travels towards the target, while updating the expected target location and employing strategy along the way using the sonar information. A mission is deemed successful when the pursuer travels within a set radius of the evading craft. The idea behind this game theory approach is that a probability of success of a given AUV over a range of missions can be determined. Furthermore, a set of design metrics can be measured, a design objective can be computed, and a merit function can be computed.

The model is coupled with the ARL's AUV problem as a system analysis before each set of simulations to determine the torpedo design parameters and sizings. Specifically, weights and available power of subsystems and components, efficiencies based on propulsor types, sonar configurations, and various other subsystems can be optimized.

Computing the probability that the AUV is successful, requires the simulation to be run many times and therefore is computationally expensive. Also, since the objective function is based at least in part on a discrete outcome, hit or miss, this function is not as smooth as most optimizers require. To address both of these issues a surrogate model is constructed using a Kriging aproximation.[1]

In this paper, we address the dynamics model, its derivation, the simulation scenarios used to extend the AUV problem, and the subsequent optimization of the AUV based on performance. The new dynamics-based AUV model and its simulation will be referred to as the *d-AUV* model.

II. AUV Model

The pursuing underwater vehicle is the dynamically modeled vehicle that pursues the evading vehicle by employing guidance control and strategy. The following assumptions are used in this simulation regarding the performance of the modeled vehicle:

1. Rigid body with equal mass distribution
2. No environmental disturbances
3. Constant gravity at any depth

4. Constant density of the surrounding medium
5. Constant thrust propulsion
6. Neutral buoyancy

In each simulation sequence, the pursuing vehicle starts at a specified initial position with a given initial velocity as if it were launched from a defending vessel. In this section, the derivation of the dynamics of AUV model are described.

A. Body Configuration

The model is based in the body-fixed frame of the AUV. Furthermore, the origin of the body-fixed frame coincides with the Center of Gravity (CG) of the vehicle body. Therefore, the CG of vehicle is always at (0,0,0).

The vehicle modeled is assumed to have a hull that is symmetric about the xy- and xz- planes, with two rudders and two elevators. Therefore, it can be assumed that the body-fixed frame coordinate system is the principal axes of inertia at the CG. By doing this, the inertia tensor is reduced to the principle moments of inertia: I_{xx}, I_{yy}, and I_{zz}.

A diagram of the current model configuration is shown in Figure 1.

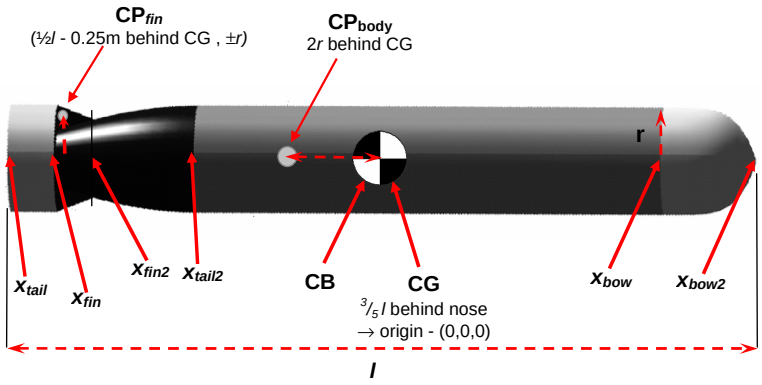

Figure 1. Vehicle Body Configuration

To further simplify the moments of inertia calculation, the vehicle cross-products of inertia, I_{xy}, I_{xy}, and I_{xy}, are assumed to be small and the vehicle is modeled as a cylinder. The body's Center of Pressure (CP) is placed one body diameter behind the CG for stability. Per the assumption of neutral buoyancy, the Center of Buoyancy (CB) is placed at the CG.

The shape or radius, $R(x)$, of this AUV model is based on the model shape[10] and is parameterized by the following terms. The nose section is defined by,

$$R(x)_{nose} = r\left[1 - \left(\frac{x-a}{a}\right)^2\right]^{\frac{1}{n}}, \quad \text{for } x_{bow} < x < x_{bow2}. \tag{1}$$

The main body section is simply,

$$R(x)_{body} = r, \quad \text{for } x_{tail2} < x < x_{bow}. \tag{2}$$

The tail section shape is described by,

$$R(x)_{tail} = \frac{1}{2}r - \left[\frac{6r}{2c^2} - \left(\frac{\tan\lambda}{c}\right)^2\right](x-l)^2 + \left[\frac{2r}{c^3} - \frac{\tan\lambda}{c^2}\right](x-(a-b))^3, \quad \text{for } x_{tail} < x < x_{tail2}. \tag{3}$$

where,

$$\begin{aligned} a &= x_{bow2} - x_{bow} \\ b &= x_{bow} - x_{tail2} \\ c &= x_{tail2} - x_{tail} \end{aligned}$$

The parameter n is an exponential parameter that can be varied to give different body shapes and is the included angle at the tip of the tail.

B. Equations of Motion

The model developed uses six degrees-of-freedom equations of motion using an Euler angle representation for the orientation of the body in space. The modeled equations of motion are:

$$\Sigma F_{ext} = m \left\{ \begin{array}{c} \dot{u} + qw - vr \\ \dot{v} + ru - pw \\ \dot{w} + pv - qu \end{array} \right\}_{\hat{b}} \tag{4}$$

$$\Sigma M_{ext} = \left[\begin{array}{ccc} I_{xx} & 0 & 0 \\ 0 & I_{yy} & 0 \\ 0 & 0 & I_{zz} \end{array} \right] \left\{ \begin{array}{c} \dot{p} \\ \dot{q} \\ \dot{r} \end{array} \right\}_{\hat{b}} + \left| \begin{array}{ccc} \hat{b}_1 & \hat{b}_2 & \hat{b}_3 \\ p & q & r \\ I_{xx}p & I_{yy}q & I_{zz}r \end{array} \right| \tag{5}$$

When these equations are combined with the equations for the forces and moments on the vehicle, the full nonlinear equations of motion for the modeled AUV are obtained.

C. External Forces and Moments

The body forces and moments typically experienced by an underwater vehicle include hydrodynamic damping along with hydrostatic and propulsive forces and moments. As a simplification, we ignore force terms that are greater than the second order in this model, since they are relatively insignificant.

1. *Hydrodynamics*

The hydrodynamics of the AUV control surfaces as well as the hull must be considered. This AUV model includes two rudders and two elevators. The Figure 2 illustrates the parameters that will be used in the determination of hydrodynamic forces.

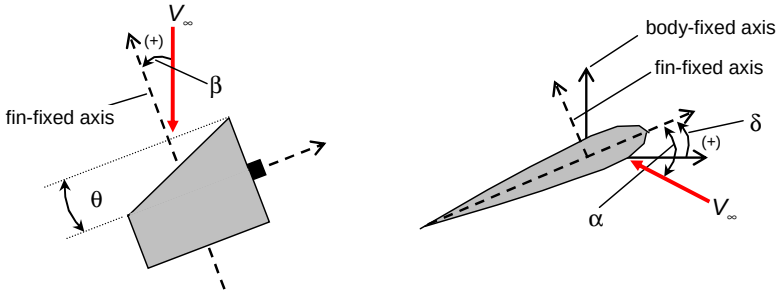

Figure 2. Control surface schematic

In order to calculate the lift and parasite drag forces, the velocity of each fin CP in body-fixed axis is calculated,

$$V_{CP\hat{b}} = V_b + \omega \times r_{CP} \tag{6}$$

where ω is the angular velocities of the body and r_{CP} is the position vector of the CP of the fin, hull, or body in the body-fixed frame. Equation 6 can be re-written as:

$$\left\{ \begin{array}{c} u \\ v \\ w \end{array} \right\}_{CPb} = \left\{ \begin{array}{c} u \\ v \\ w \end{array} \right\} + \left| \begin{array}{ccc} \hat{b_1} & \hat{b_2} & \hat{b_3} \\ p & q & r \\ x_{CP} & y_{CP} & z_{CP} \end{array} \right| \tag{7}$$

where (x_{CP}, y_{CP}, z_{CP}) specifies the location of the CP of a control surface or the hull.

The velocity of each control surface must be transformed from the body-fixed frame to the the fin-fixed frame to calculate lift and drag. To do this we need to transform the velocity of each fin CP. Using these velocity components, the angle of attack α, and sideslip angle β of each control surface is calculated using,

$$\alpha_{fin} = \tan^{-1}\left(\frac{w_{fin}}{u_{fin}}\right) \tag{8}$$

and

$$\beta_{fin} = \sin^{-1}\left(\frac{-v_{fin}}{V_{fin}^2}\right) \tag{9}$$

where,

$$V_{fin}^2 = \sqrt{u_{fin}^2 + v_{fin}^2 + w_{fin}^2}. \tag{10}$$

Finally, using these values, lift and drag can be calculated. This is a straight forward calculation for the hull body in the body-fixed frame, although for each control surface, the body forces must be rotated from the fin-fixed frame to the body-fixed frame.
In this model, symmetric airfoils are assumed for the control surfaces. For this model, airfoil data (c_L versus α and c_L versus c_D) from Bottaccini[13] is utilized using the standard equations.

2. Nonlinear Effects

The nonlinear dynamics terms are now considered. By assuming that the fundamental component of **rolling resistance**, or rolling drag, is from cross-flow drag of the control surfaces, we estimated the rolling resistance using the following equation:[10]

$$L_{p|p|} = Y_{vv} r_{mean}^3 \tag{11}$$

where Y_{vvf}, is the fin component of cross-flow drag coefficient, and is the mean fin height above the vehicle center line. According to Prestero,[10] Y_{vvf} is at best a rough approximation for the actual value, and that experimental data is more appropriate.

Added mass is a measure of the mass of the moving water ahead of an underwater vehicle when the vehicle accelerates. The added mass terms on hull in the vehicle's axial direction, along with the fin contribution in the other directions. The axial added mass can be estimated by approximating the vehicle hull shape as an ellipsoid where the major axis is half of the vehicle length l and the minor axis is half of the vehicle diameter, or the radius r. The following empirical formula is used to calculate the added axial mass of an ellipsoid:

$\mathbf{F_x}$:

$$F_x = X_{\dot{u}} \dot{u} \tag{12}$$

where,

$$X_{\dot{u}} = \frac{4\chi\rho\pi}{3}\frac{l}{2}r^2 \tag{13}$$

The parameter χ is empirically determined by the ratio of the vehicle to the diameter. For the model, we take the empirical values of the REMUS vehicle present by Prestero[10] and given in Table 1.

$\frac{l}{d}$	χ
0.1	0.148
0.2	3.008
0.4	1.428
0.6	0.9078
0.8	0.6514
1.0	0.50
1.5	0.3038
2.0	0.210
2.5	0.1583
3.0	0.1220
5.0	0.05912
7.0	0.03585
10.0	0.02071

Table 1. $\frac{l}{d}$ versus χ

Crossflow added mass is calculated using a more detailed model of the vehicle. Using strip theory, the added mass per unit length of a cylindrical hull cross section is expressed as:[10]

$$m_a(x) = \pi\rho R(x)^2 \tag{14}$$

The added mass of a circle with fins is given as:[10]

$$m_{af} = \pi\rho\left(a_{fin}^2 - R(x)^2 + \frac{R(x)^4}{a_{fin}^2}\right) \tag{15}$$

where a_{fin} is the maximum height of the vehicle's fins above the centerline. Finally, we can calculate the following equations for crossflow added mass.

$\mathbf{F_y}$:

$$F_y = Y_{\dot{v}}\dot{v} \tag{16}$$

where,

$$Y_{\dot{v}} = -\int_{x_{tail}}^{x_{fin}} m_a(x)dx - \int_{x_{fin}}^{x_{fin2}} m_{af}(x)dx - \int_{x_{bow}}^{x_{fin2}} m_a(x)dx \tag{17}$$

$\mathbf{F_z}$:

$$F_z = Z_{\dot{w}}\dot{w} + Z_{\dot{q}}\dot{q} \tag{18}$$

where,

$$\begin{aligned} Z_{\dot{w}} &= Y_{\dot{v}} \\ Z_{\dot{q}} &= \int_{x_{tail}}^{x_{fin}} xm_a(x)dx - \int_{x_{fin}}^{x_{fin2}} xm_{af}(x)dx - \int_{x_{bow}}^{x_{fin2}} xm_a(x)dx \end{aligned} \tag{19}$$

Rolling added mass is estimated by assuming the vehicle hull surface does not generate any added mass in roll, and neglect the added mass generated by any small protuberances.[10] Therefore, we only consider the hull section containing the control surfaces. Thus, the rolling added mass of a circle with fins is defined by the following empirical formula:

L :

$$L = L_{\dot{p}}\dot{p} \tag{20}$$

where,

$$L_{\dot{p}} = \int_{x_{fin2}}^{x_{fin}} \frac{2}{\pi} a_{fin}^4 dx \tag{21}$$

where a_fin is the fin height above the vehicle centerline. The crossflow added mass movement contributions are again calculated using strip theory:

M :

$$M = M_{\dot{w}}\dot{w} + M_{\dot{q}}\dot{q} \tag{22}$$

where,

$$M_{\dot{q}} = -\int_{x_{tail}}^{x_{fin}} x^2 m_a(x)dx - \int_{x_{fin}}^{x_{fin2}} x^2 m_{af}(x)dx - \int_{x_{fin2}}^{x_{bow2}} x m_a(x)dx \tag{23}$$
$$M_{\dot{w}}\dot{w} = Z_{\dot{q}}\dot{q}$$

N :

$$N = N_{\dot{v}}\dot{v} + N_{\dot{r}}\dot{r}, \tag{24}$$

where,

$$\begin{aligned} N_{\dot{v}} &= -M_{\dot{w}} \\ N_{\dot{r}} &= M_{\dot{q}} \end{aligned}$$

The remaining cross-terms are a consequence of added mass coupling. The following equations define the added mass cross terms for each force component.

$\mathbf{F_x}$:

$$F_x = X_{wq}wq + X_{qq}qq + X_{vr}vr + X_{rr}rr \tag{25}$$

where,

$$\begin{aligned} X_{wq} &= Z_{\dot{w}} \\ X_{qq} &= Z_{\dot{q}} \\ X_{vr} &= -Y_{\dot{v}} \\ X_{rr} &= -Y_{\dot{r}}. \end{aligned}$$

$\mathbf{F_y}$:

$$F_y = Y_{ur}ur + Y_{wp}wp + Y_{pq}pq \tag{26}$$

where,

$$\begin{aligned} Y_{ur} &= X_{\dot{u}} \\ Y_{wp} &= -Z_{\dot{w}} \\ Y_{pq} &= -Z_{\dot{q}}. \end{aligned}$$

$\mathbf{F_z}$:

$$F_z = Z_{uq}uq + Z_{vp}vp + Z_{rp}rp \tag{27}$$

where,

$$\begin{aligned} Z_{uq} &= -X_{\dot{u}} \\ Z_{vp} &= Y_{\dot{v}} \\ Z_{rp} &= Y_{\dot{r}} \end{aligned}$$

The following equations define the added mass cross terms for each moment component.

$\mathbf{L}$:

$$L = 0 \tag{28}$$

$\mathbf{M}$:

$$M = M_{uq}uq + M_{vp}vp + M_{rp}rp, \tag{29}$$

where,

$$\begin{aligned} M_{uq} &= -Z_{\dot{q}} \\ M_{vp} &= -Y_{\dot{r}} \\ M_{rp} &= K_{\dot{p}} - N_{\dot{r}}. \end{aligned}$$

$\mathbf{N}$:

$$N = N_{ur}ur + N_{wp}wp + N_{pq}pq \tag{30}$$

where,

$$\begin{aligned} N_{ur} &= -Y_{\dot{r}} \\ N_{wp} &= Z_{\dot{q}} \\ N_{pq} &= -(K_{\dot{p}} - M_{\dot{q}}). \end{aligned}$$

Crossflow drag is considered to be the summation of the hull and fin crossflow drag forces. The strip theory method used for calculating to the hull drag is similar to strip theory described by Prestero.[10] The following equations define the cross-flow drag for each force component.

$\mathbf{F_x}$:

$$F_x = 0 \tag{31}$$

$\mathbf{F_y}$:

$$F_y = Y_{v|v|}v|v| + Y_{r|r|}r|r| \tag{32}$$

where,

$$Y_{v|v|} = -\frac{1}{2}\rho c_{dc}\int_{x_{tail}}^{x_{bow2}} 2R(x)dx - 2\left(\frac{1}{2}\rho S_{fin}c_{dc}\right) \tag{33}$$

and

$$Y_{r|r|} = -\frac{1}{2}\rho c_{dc}\int_{x_{tail}}^{x_{bow2}} 2x|x|R(x)dx - 2x_{fin}|x_{fin}|\left(\frac{1}{2}\rho S_{fin}c_{dc}\right) \tag{34}$$

F$_z$:

$$F_z = Z_{w|w|}w|w| + Y_{q|q|}q|q| \tag{35}$$

where,

$$\begin{aligned} Z_{w|w|} &= Y_{v|v|} && (36)\\ Z_{q|q|} &= Y_{r|r|}. && (37)\\ & && (38) \end{aligned}$$

The cross-flow drag coefficient of a cylinder, c_{dc}, in (33) and (34) can be estimated as 1.1, and the cross-flow drag coefficient, c_{df}, can be expressed using the following equation:[10]

$$c_{df} = 0.1 + 0.7t \tag{39}$$

where t is the ratio of the widths of the top and bottom of the fin along the vehicle x-axis (fin taper ratio). The following equations define the cross-flow drag for each moment component.

L :

$$L = 0 \tag{40}$$

M :

$$M = M_{w|w|}w|w| + M_{q|q|}q|q| \tag{41}$$

where,

$$\begin{aligned} M_{w|w|} &= -N_{v|v|}\\ M_{q|q|} &= N_{r|r|}. \end{aligned}$$

N :

$$N = N_{v|v|}v|v| + N_{r|r|}r|r| \tag{42}$$

where,

$$\begin{aligned} N_{v|v|} &= -M_{w|w|}\\ M_{r|r|} &= -M_{q|q|}. \end{aligned}$$

3. Propulsion

As mentioned above, it is assumed that a simple propulsion system is employed; a constant propulsive force, thrust, is used throughout the simulation. Thus,

$$F_{propulsion} = \begin{bmatrix} T \\ 0 \\ 0 \end{bmatrix} \tag{43}$$

where T is thrust. In this model, we assume that no rolling moment caused by the propeller.

4. Hydrostatics

The gravitational force on the vehicle is transformed from the inertial frame to the body-fixed frame as shown in the following equation:

$$F_{gravity} = mg \begin{bmatrix} -\sin(\theta) \\ \sin(\phi)\cos(\theta) \\ \cos(\phi)\cos(\theta) \end{bmatrix} \tag{44}$$

The buoyancy force acts at the Center of Buoyancy. This force on the vehicle also must be transformed from the inertial frame to the body-fixed frame:

$$F_{buoyancy} = -pVg \begin{bmatrix} -\sin(\theta) \\ \sin(\phi)\cos(\theta) \\ \cos(\phi)\cos(\theta) \end{bmatrix} \tag{45}$$

where is the density of the surrounding fluid and V is the volume the vehicle. Again, in our model we assume a cylindrical shape.

D. Sonar

A simplistic form of sonar is implemented in the model that is based on the sonar subsystem used in the ARL AUV model. The inputs are the velocity and position of the target in the inertial frame. The function of the implemented sonar subsystem is guidance and tracking. This is accomplished by an acoustic array that generates a signal pattern composed of one or more detection beams contained within a rectangular field of view (FOV). In the AUV model, if the target is detected within the FOV, it is assumed that one of the detection beams can track its position.

Within this subsystem the position of the target is first subtracted from the pursuing vehicles position in inertial frame-based coordinates. This position and the target's velocity are rotated to the pursuing vehicle's body-fixed frame. Subsequently, the position of the target is viewed by the pursuing vehicle with respect to its body-fixed reference frame.

In order to imitate the sonic waves emitted from a sonar transmitter at the beginning of each detection cycle, the model keeps track of the position of the 'signal' that defines each region as it propagates. Each signal position is expressed by the following:

$$\begin{bmatrix} x_{beam} \\ y_{beam} \\ z_{beam} \end{bmatrix} = V_{sound}t \begin{bmatrix} \cos\left(\frac{\gamma_h}{2}\right) \\ \sin\left(\frac{\gamma_h}{2}\right) \\ \sin\left(\frac{\gamma_v}{2}\right) \end{bmatrix} \tag{46}$$

where γ_h and γ_v are the horizontal and vertical FOV respectively specified in degrees.

E. Control System

The model utilizes a simple tracking control system that uses proportional-integral (PI) control. The integral control is added to reduce steady-state error. The tracking error is calculated between the evader's position relative to the pursuer as measure by a sonar subsystem.

1. Strategy - Lead Pursuit Path

The strategy defines the path, or positions, input in to each controller for pursuit. This subsystem implements the strategy used by the pursuing underwater vehicle for tracking down the evader. The concept of this strategy is simple: predict the path of a moving target by aiming ahead of it. This module uses the target position and velocity outputs from the sonar subsystem as its inputs. The velocity component is scaled and added to the current target position to obtain the lead. This scaling is dependant on the vehicle's distance from its target. It is defined by the following:

$$\begin{bmatrix} x_{lead} \\ y_{lead} \\ z_{lead} \end{bmatrix} = C_i\sqrt{x_{rel}^2 + y_{rel}^2 + z_{rel}^2} \cdot \begin{bmatrix} V_{y,x} \\ V_{t,y} \\ V_{t,z} \end{bmatrix} \tag{47}$$

where,

$$x_{rel} = x_t - x_p \tag{48}$$
$$y_{rel} = y_t - y_p \tag{49}$$
$$z_{rel} = z_t - z_p. \tag{50}$$

The pursuing vehicle's position (x_p, y_p, z_p) is always (0,0,0) since the frame of reference is body fixed relative to its center of gravity. Therefore, as the pursuer moves closer to its target, the lead is gradually attenuated, thus reducing the chance of overshooting it. The parameter C is comparable to a gain. In the strategy employed, C can take two values, C_1 or C_2, depending on the relative distance of the evader from the pursuing vehicle. The resulting new positions become the inputs on which the rudder and elevator controllers direct the vehicle.

$$\begin{bmatrix} x_t^{'} \\ y_t^{'} \\ z_t^{'} \end{bmatrix} = \begin{bmatrix} x_t \\ y_t \\ z_t \end{bmatrix} + \begin{bmatrix} x_{t,lead} \\ y_{t,lead} \\ z_{t,lead} \end{bmatrix} \tag{51}$$

III. Optimization of the AUV

Using the dynamics model of the AUV presented in this paper, optimization can be performed to design a AUV based on its performance for a given mission. The details of the optimization process are explained in this section.

A. Mission Details

To optimize the performance of the AUV model, it is simulated using a game theory approach. In these simulations, we define the craft described in this paper as the pursuing craft. A trajectory of a second craft, defined as the evader, is also simulated using simple linear equations. This is done to reduce the computing time. Therefore, it is an unintelligent representation of a moving target that does not intelligently evade its opponent, whereas the pursing AUV intelligently pursues this target.

In each mission, the evader travels along a path that ultimately ends at its target, while the pursuing AUV starts from this target, tracks, and attempts to hit the pursuing vessel before it reaches its destination. Idealistically, this is a simulation of a submarine defending itself against an incoming torpedo by firing an 'anti-torpedo' torpedo as a countermeasure. Multiple attack scenarios are executed within each set of simulations.

More specifically, these scenarios entail various maneuvers used by the evader to unintelligently evade the pursuer at different positions of attack (angle and depth) and different speeds of the evader. These different orientations are illustrated in Figure 3. Due to symmetry, the oncoming torpedo needs only to be positioned on one side of the semicircle that is defined by the radius around the evader's target (which can also been seen as the pursuer's starting point). At the start of each simulation, the pursuer is given the initial position of the evader.

The evader model includes four path scenarios: a (1) straight line path, (2) barrel roll maneuver, (3) curved trajectory, and (4) weaving path. These paths are modeled using simple line and sinusoid equations. These paths are shown in Figure 4, where (1) and (2) are climbing towards the pursuer and defended vessel, and (3) and (4) attack from the same depth. To further simplify the dynamics of the evading vehicle paths, the evader begins at the origin, although the end result of the simulation given an initial orientation and position for the pursuer is as if the evading vehicle is starting at varied positions.

In addition to varying starting orientation, the speed, the height from which the evading vehicle attacks, and the path type make up the possible simulation scenarios can each be varied. The performance of the

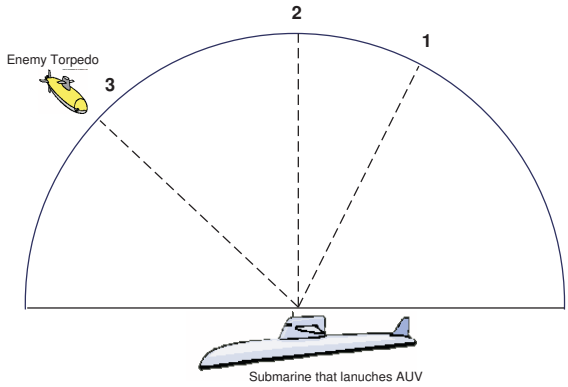

Figure 3. Mission scenarios

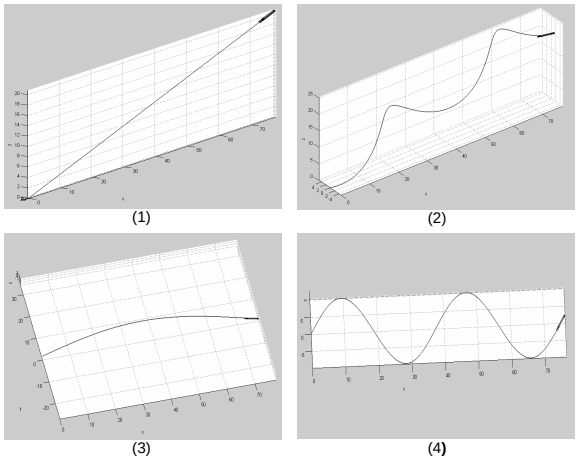

Figure 4. The evader's paths

pursuing vehicle based on the percentage of hits and average minimum encounter distance (for misses) for the scenarios mentioned. This is what makes up the objective function to be optimized. The motivation behind these simulated mission is to test the AUV under the actual scenario that a real AUV may encounter.

B. Problem Statement

The ARL at Penn State required a more complex AUV problem to be developed for unclassified AUV design. Therefore, the d-AUV model was developed to add complexity to a relatively simplistic sizing model the ARL had developed. The d-AUV model is coupled to the ARL's original AUV model as a system analysis call for componential sizings before each set of simulations are executed.

For each set of simulations, three metrics are stored: (1) the number of successful 'hits' by the pursuer of the evader, (2) the average minimum separation distance during each mission, and (3) the time required for each mission. Each of these metrics is assigned a weight factor, -50, 2.5 and 2.5 respectively. Noting the sign convention, we wish to maximize the probability of success of the AUV while minimize the minimum distance separation and mission time. Although the assignment of these weights deserves more study, the factors used are suitable for this paper.

The objective is to achieve an increase the probability of success for a given mission, while reducing the time for each mission for quicker strike. Furthermore, if the AUV is unsuccessful in it's attempt, it should travel

as close as possible to the evading vessel.

C. Optimization Methodology and Results

The initial problem, developed at the ARL for external release, was a simple linear two variable design problem. By adding dynamics and a control system, the new problem includes seven more design parameters: four control gains and three strategy parameters.

On average, using a computer with a Pentium 4 1.8 GHz processor, each d-AUV objective function call requires approximately 12-14 minutes depending upon the given design and simulation scenario. Furthermore, because of the noisiness of the design space, local finite differencing becomes unreliable requiring longer optimization trials for gradient-based algorithms. For example, using MATLAB's Sequential Quadratic Programming (SQP) algorithm, *fmincon*, 691 function calls were required. This optimization took approximately 139 hours to complete.

Because of the computational expense and noise in the objective function, it was advantageous to construct a Kriging model to approximate the design space. The kriging model was constructed using 338 samples uniformly distributed throughout the design space. The number of samples was determined by taking four times the number of sample point suggested by Jin *et al*.[14] Kaufmann *et al*[15] suggests that $1.5k$ sample points be used for 5-10 variable problems. The parameter k is given by,

$$k = \frac{(n+l)(n+2)}{2}, \tag{52}$$

for n design variables. Using this surrogate model, we again applied MATLAB's *fmincon*.

For each simulation used for this paper, the evader starts from each of 3 different yaw positions relative to the submarine located on a 150 meter semi-circle as seen in Figure 3. The yaw angles used here are also shown in Figure 3. From each of these yaw positions three different starting height of the torpedo are used one is level with the submarine and the other two are 10 meters above and below submarine. Two more variations are used for each of these spacial starting points and those are the evading maneuvers used by the torpedo and also the speed at which the torpedo can travel. Four different evading maneuvers were used: straight path to the submarine, barrel rolling path, a half-sinusoidal path, and a two dimensional weave in the plane of the submarine. The evading torpedo was also given two speeds which were held constant for a single simulation these speeds were $10\frac{m}{s}$ and $25\frac{m}{s}$. The 3 starting yaws, 3 heights, 4 paths, and 2 different speeds result in 72 different simulation runs. For each simulation if the AUV comes within a radius of twice its length to the torpedo it is considered a successful mission. If the torpedo evades the AUV and hits the submarine the run is considered a failed mission. In either case the total simulation time to either hit or miss and also the closest encounter distance are calculated. The final results for the optimization run on the actual model and approximated kriging model are presented in Table 2. The global minimum of this problem is not currently known. The performance metric at the both solutions, are displayed in Table 3.

From the resulting values, it is shown that the design with the higher probability of success yields the higher objective value. Since probability of success is generally viewed as the most important measure of performance, the weight factors currently in use may not be suitable. In further work a Pareto curve could be generated for different weightings of the multiobjective merit function. Furthermore, in Table 2 it is shown that for the kriging surrogate model of the design space, an optimum design is found with an objective value of -32.7193, where the actual objective value at the design is -4.0759. This large discrepancy calls the predictability of the kriging model of the actual d-AUV design space into question.

Design variable	Variable name	Initial design	Exact Model solution	Kriging Model solution
x_l	payload length	1.5	1.612	1.7103
x_2	thrust	16,000	13,067	17,000
x_3	rudder P gain	0.9	1.061	1.0351
x_4	rudder I gain	0.1	0.184	0.10184
x_5	elevator P gain	0.9	0.7	0.7339
x_6	elevator I gain	0.1	0.213	0.077203
x_7	strategy - lead distance	20	26.999	22.041
x_8	strategy - C_1	0.2	0.028	0.015221
x_9	strategy - C_2	0.2	0.0121	0.017383
f^*	-	269.2	-19.4478	-32.7193†
Function calls	-	-	691	338
CPU Time (hrs)	-	-	139	77

† exact f^*=-4.0759.

Table 2. SQP optimization of exact and approximated design for the AUV problem

Performance metric	Weight factor	Initial design	Exact Model solution	Kriging Model solution
Probability of Success	-50	0.0147	0.639	0.653
Pursuit Minimum Separation	2.5	8.025 m	4.896 m	4.724 m
Pursuit Time	2.5	19.189 s	5.937 s	7.924 s
f^*		269.2	-19.4478	-32.7193

Table 3. Performance results from simulation sets at optimum solutions

IV. Conclusions and Future Work

A more complex AUV problem has been developed. The new d-AUV model that has been developed incorporates a dynamics-based game theory simulation, where the ARL AUV model provides design parameters as a system analysis call before each simulation. The inclusion of nonlinear dynamics to the problem results in a more realistic and suitable model for design-based optimization. This is advanced with the addition of performance-based metrics as part of the design optimization process.

To further this work, we will implement optimal control in conjunction with game theory. Furthermore, currently only a tracking control system has been implemented. However, the AUV's tendency to roll requires that a regulator system also be implemented to keep roll angle, θ, and roll rate, p zero. These changes should add to the robustness of the model. Also, the discrete variables that can be varied within the ARL Penn State AUV model must be optimized using a non-gradient based optimization method such as a genetic algorithm.

Acknowledgments

This research effort was supported in part by the following grants and contracts: ONR Grant N00014-02-1-0786, NSF Grant DMI-0114975, and a Grant from the AFRL / DARPA through Anteon Corporation contract F33615-98-D-3210.

References

[1]Martin, J.D., Simpson, T.W.: *A Study on the Use of Kriging Models to Approximate Deterministic Computer Models*, Proceedings of ASME 2003 Design Engineering Technical Conferences and Computers and Information in Engineering Conference, DET2003/DAC-48762, Chicago, IL, September 2-6, 2003.

[2]Isaacs, R.: *Differential Games*, Dover Edition, 1965.

[3]Yukish, M., Bennett L., Simpson, T.W.: *Requirements on MDO Imposed By the Undersea Vehicle Conceptual Design Problem*, Proceedings of the 8th AIAA/USAF/NASA/ISSMO Symposium on Multidisciplinary Anaylsis and Optimization, AIAA-2000-4816, Long Beach, CA, September 6-8, 2000.

[4]Belegundu, A.D., Halberg E., Yukish,M., Simpson, T.W.: *Attribute-Based Multidisciplinary Optimization of Undersea Vehicles*, Proceedings of the 8th AIAA/USAF/NASA/ISSMO Symposium on Multidisciplinary Anaylsis and Optimization, AIAA-2000-4816, Long Beach, CA, September 6-8, 2000.

[5]Breslin, J.P., Anderson, P.: *Hydrodynamics of Ship Propellers*, Cambridge University Press, 1994.

[6]Gearhart, W.S., Hamblin, A.L.: *The Propeller and its Derivatives*, Applied Research Laboratory Technical Memorandum File No. 87-197, 1987.

[7]Hoerner, S.H.F., Borst, H.V.: *Fluid-Dynamic Lift, Hoerner Fluid Dynamics*, 1985.

[8]Kurdila, A., Dzielski, J., Lind, R.: *Modeling and Control of a Class of Underwater Missiles*, August 26, 2001.

[9]Kou, B.C.: *Automatic Control Systems*, 5th ed, Prentice Hall Inc, 1987.

[10]Prestero, T.: *Verification of a Six-Degree of Freedom Simulation Model for the REMUS Autonomous Underwater Vehicle*, Masters Thesis, University of California at Davis, 2001.

[11]Pérez, V. M., Renaud, J.E., Watson, L. T.: *Adaptive Experimental Design for Construction of Response Surface Approximations*, Proceedings of the 42st AIAA/ASME/ASCE/AHS/ASC Structures, Structural Dynamics, and Materials Conference, AIAA 2001-1622, Seattle, WA, April 16-19, 2001.

[12]Vanderplaats, G.N.: *Numerical Optimization Techniques for Engineering Design*, McGraw-Hill, 1984.

[13]Bottaccini, M.R.: *The Stability Coefficients of Standard Torpedoes.*, July 18, 1954.

[14]Jin,R., Chen,W., Simpson, T.W.: Comparative studies of metamodelling techniques under multiple modelling criteria., *Structural and Multidisciplinary Optimization*, 2001.

[15]Kaufmann, M.,Balabanov, V.: Burgee, S.L., Giunta, A.A., Grossman, B., Mason, W.H., Watson, L.T., *Variable Complexity response surface approximations for wing structural weight in the HSCT design.* Proc. 34th Aerospace Sciences Meeting and Exhibit, AIAA Paper 96-0089, 1996.